Radiative proton-deuteron capture in a gauge invariant relativistic model

A. Yu. Korchin,[1,*] D. Van Neck,[1] O. Scholten,[2] and M. Waroquier[1]
[1]*Department of Subatomic and Radiation Physics, University of Gent, Proeftuinstraat 86, B-9000 Gent, Belgium*
[2]*Kernfysisch Versneller Instituut, Zernikelaan 25, 9747 AA Groningen, The Netherlands*
(Received 19 October 1998)

A relativistic model is developed for the description of the process $p+d\leftrightarrow{}^3\mathrm{He}+\gamma^*$. It is based on the impulse approximation, but is explicitly gauge invariant and Lorentz covariant. The model is applied to radiative proton-deuteron capture and electrodisintegration of ^{3}He at intermediate energies. Results for cross sections and vector and tensor analyzing powers are presented. [S0556-2813(99)03504-9]

PACS number(s): 21.45.+v, 25.40.Lw, 25.20.−x

I. INTRODUCTION

Considerable progress has been achieved up to now in theoretical studies of radiative proton-deuteron capture and the reverse process of the photodisintegration of ^{3}He in the nonrelativistic framework. Being limited in space we mention here only several studies. Calculations including only the nucleon Born term [1,2] were not succesful in explaining the *pd* capture data, whereas other calculations [3–5] were restricted to low energies. In [6–8] the effects of different realistic nucleon-nucleon potentials were investigated. More references can be found in a recent review article [9]. An alternative approach was developed in [10], in which only selected terms for the amplitude were taken into account. It included contributions of meson exchange currents (MEC) and the *pd* interaction explicitly, and these were found to be important. Although more phenomenological in its approach, this allowed for reasonably accurate estimates for the cross sections at high energies.

One of the main ingredients in the description of the capture process is the nuclear electromagnetic (e.m.) current. In most calculations it is chosen in the impulse approximation; i.e., it is the sum of the e.m. currents for the free nucleons. Therefore the requirement of gauge invariance is, in general, not fulfilled. Siegert's theorem is often applied, as it allows one to express part of the electric transitions through the one-body charge density operator, thereby reducing considerably the complexity of the problem. This approach has also been used in the recent Faddeev calculations reported in [11,12]. With increasing photon energy, however, this method becomes less adequate and one is forced to include explicitly all contributions to the e.m. current.

Another aspect of the capture reactions at intermediate energies is the large value of the momenta of the involved particles. For example, at a proton energy of about 200 MeV one probes the wave function (WF) of ^{3}He at momenta of about 350 MeV, implying that relativistic corrections may be appreciable.

In this paper we develop a covariant model for the reaction $p+d\leftrightarrow{}^3\mathrm{He}+\gamma^*$, where γ^* is a real or virtual (spacelike) photon, at proton energies of up to a few hundred MeV. Special attention is paid to the construction of a conserved e.m. current. It is known that at small photon energies the reaction amplitude is dominated by radiation from the external proton, deuteron, and ^{3}He legs, and this consideration led to the development of low-energy theorems (LETs). For bremsstrahlung in scattering of charged particles, the LET was derived by Low [13]. For deuteron photodisintegration the LET was established by Sakita [14], and later on extended [15] to other light nuclei. These LETs are based on an expansion of the amplitude in powers of the photon energy E_γ and on gauge invariance.

In kinematical conditions where the photon energy is not small one may still assume the dominance of the above external amplitude, however, without applying the expansion in E_γ. Imposing gauge invariance restricts to a large extent the so-called internal contributions which are not explicitly present in the external amplitude. We suggest a method to construct the internal amplitude which accounts for a part of MEC and *pd* rescattering, and converges to the LET at small photon energies.

In our approach we start from the covariant model of [16], which was developed for low-energy radiative *pd* capture. Aiming at higher energies we supplement this model by the internal amplitude, which turns out to give a sizable contribution at all energies considered. An important input in the model is the pd^3He vertex function, for which recent calculations [17–19] of the ^{3}He WF are used.

The amplitude obtained in this way may be called a gauge-invariant relativistic impulse approximation. In this amplitude propagators of all particles are taken as free propagators, which might not be appropriate for composite particles like ^{3}He or *d*. To improve on this we study the effect of self-energy corrections to the ^{3}He propagator. This appears to be important in the capture cross section at energies of about 200 MeV. The resulting amplitude still has the shortcoming of being purely real. To account for the unitarity requirement we include the *pd* scattering phase shifts in the channel $J^P=\frac{1}{2}^+$, which generate the imaginary part of the amplitude. The latter is crucial for the proton analyzing power A_y in *pd* capture. The phase shifts are included in such a way that gauge invariance is preserved. The rescattering in the $\frac{3}{2}^-$ channel is approximately taken into account via an excited state of the ^{3}He.

The model is tested for capture cross sections, and proton and deuteron analyzing powers. We also extend the model to

*Permanent address: National Science Center ''Kharkov Institute of Physics and Technology,'' 310108 Kharkov, Ukraine.

virtual (spacelike) photons and calculate the electrodisintegration of ^{3}He in the kinematical conditions of NIKHEF and Saclay experiments where either the proton or the deuteron is detected in concidence with the electron. Calculations within the same framework for the case of virtual photons in the timelike regime, i.e., e^+e^- production in pd capture, have been presented earlier [20].

We should mention that the so-called field-theory approach for photonuclear reactions was suggested earlier in [21] and applied in [22] for the ^{3}He photodisintegration. This relativistic formulation is somewhat similar to our model and also includes radiation from p, d, and ^{3}He. The method for constructing the internal amplitude (called the contact term in [22]) and its explicit structure is, however, different.

The outline of the paper is as follows. In Sec. II we describe the model for the $pd\leftrightarrow{}^3\mathrm{He}\gamma^*$ reaction. The consequences of gauge invariance are considered and the internal amplitude is derived. The relations between the relativistic pd^3He vertex function and the nonrelativistic WF of ^{3}He are also discussed. In Sec. III self-energy corrections to the ^{3}He propagator and pd rescattering effects are considered. The comparison of the calculations with the radiative pd capture experiments and with Saclay and NIKHEF data for $^3\mathrm{He}(e,e'd)p$ and $^3\mathrm{He}(e,e'p)d$ reactions is presented in Sec. IV. A summary and conclusions are given in Sec. V. In Appendix A the half-of-shell e.m. vertex of the deuteron is discussed. Appendix B contains the expression for the gauge-invariant amplitude. Finally, we have collected in Appendix C the expressions for response functions, cross sections, and vector and tensor analyzing powers in terms of the matrix elements.

II. DESCRIPTION OF THE MODEL

The four-momenta of the proton, deuteron, ^{3}He nucleus, and (virtual) photon are denoted by p_1, p_2, p_3, and q respectively. The amplitude for the $pd\rightarrow{}^3\mathrm{He}\gamma^*$ reaction can be written as

$$M_{\lambda_\gamma\lambda_h,\lambda_p\lambda_d}=e\epsilon_\mu^*(\lambda_\gamma)\overline{u}(\vec{p}_3,\lambda_h)M^{\mu\alpha}u(\vec{p}_1,\lambda_p)\xi_\alpha(\lambda_d), \tag{1}$$

where e is the proton charge, $\overline{u}(\vec{p}_3,\lambda_h)[u(\vec{p}_1,\lambda_p)]$ is the spinor for ^{3}He [proton], and helicities of the particles are denoted by λ's. The polarization vectors of the photon $\epsilon_\mu(\lambda_\gamma)$ and the deuteron $\xi_\alpha(\lambda_d)$ satisfy the Lorentz condition

$$q\cdot\epsilon(\lambda_\gamma)=p_2\cdot\xi(\lambda_d)=0. \tag{2}$$

In the next subsections we will discuss different ingredients needed for constructing $M_{\lambda_\gamma\lambda_h,\lambda_p\lambda_d}$.

A. Radiation from external lines

First we consider (virtual) photon radiation from the external lines of the particles (first three diagrams of Fig. 1). The external amplitude reads

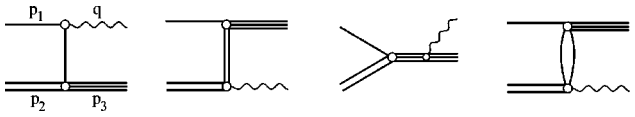

FIG. 1. Diagrams corresponding to the external amplitude.

$$\begin{aligned}M^{\mu\alpha}_{\mathrm{ext}}=&\Phi^\alpha(p_3,p_2,p_1-q)S(p_1-q,m_1)\Gamma^\mu(p_1-q,p_1)\\&+\Phi^\beta(p_3,p_2-q,p_1)\Delta_{\beta\rho}(p_2-q)\Gamma^{\rho\alpha\mu}(p_2-q,p_2)\\&+\Gamma^\mu(p_3,p_3+q)S(p_3+q,m_3)\Phi^\alpha(p_3+q,p_2,p_1),\end{aligned} \tag{3}$$

where $S(k,m)=(\not k-m+i0)^{-1}$ is the free propagator of the spin-$\frac{1}{2}$ particle with mass m and the deuteron propagator is $\Delta_{\beta\rho}(k)=(-g_{\beta\rho}+k_\beta k_\rho/m_2^2)(k^2-m_2^2+i0)^{-1}$. The structure of the $pd\rightarrow{}^3$He vertex function Φ^α will be discussed later.

We note here that in this formulation the s amplitude (third diagram in Fig. 1) takes into account the pole contribution (but not the regular contribution) of the initial-state pd interaction, and hence takes care of the problem with the orthogonality between initial and final states mentioned in [23].

For the moment we neglect explicit off-shell effects in the e.m. vertices and self-energy contributions to the propagators (in Sec. III self-energy corrections to the ^{3}He propagator are considered). Correspondingly the e.m. vertex function for spin-$\frac{1}{2}$ particles is chosen in the form

$$\begin{aligned}\Gamma^\mu(p-q,p)&=\Gamma^\mu(p,p+q)\\&=Z\gamma^\mu-i\frac{\sigma^{\mu\nu}q_\nu}{2m}F_2(q^2)\\&\quad+Z\tilde{F}_1(q^2)(q^\mu\not q-q^2\gamma^\mu),\end{aligned} \tag{4}$$

where $F_1(q^2)$ and $F_2(q^2)$ are, respectively, the Dirac and Pauli e.m. form factor (FF), $\tilde{F}_1(q^2)\equiv[1-F_1(q^2)]/q^2$, and $Z=1(2)$ for the proton (^{3}He). Note that this vertex obeys the Ward-Takahashi (WT) identity for the half-off-shell case [24].

The expression for the half-off-shell γdd vertex is more involved. It can be written as (see Appendix A for details)

$$\begin{aligned}&\Gamma^{\rho\alpha\mu}(p_2-q,p_2)\\&\quad=-g^{\rho\alpha}(2p_2-q)^\mu+(p_2-q)^\rho g^{\mu\alpha}\\&\qquad+\tilde{F}_1(q^2)g^{\rho\alpha}[q^2(2p_2-q)^\mu-q\cdot(2p_2-q)q^\mu]\\&\qquad+F_2(q^2)(q^\rho g^{\mu\alpha}-q^\alpha g^{\mu\rho})\\&\qquad+\frac{F_3(q^2)}{2m_2^2}\Big[q^\rho q^\alpha(2p_2-q)^\mu\\&\qquad-\frac{1}{2}q\cdot(2p_2-q)(q^\alpha g^{\mu\rho}+q^\rho g^{\mu\alpha})\Big],\end{aligned} \tag{5}$$

and fulfills the WT identity for the half-of-shell case:

$$q_\mu \Gamma^{\rho\alpha\mu}(p_2-q,p_2)\xi_\alpha(\lambda_d) = [\Delta^{-1}(p_2)^{\rho\alpha}-\Delta^{-1}(p_2-q)^{\rho\alpha}]\xi_\alpha(\lambda_d) = [-q\cdot(2p_2-q)g^{\rho\alpha}+(p_2-q)^\rho q^\alpha]\xi_\alpha(\lambda_d), \tag{6}$$

where $\Delta^{-1}(k)^{\rho\alpha}=(m_2^2-k^2)g^{\rho\alpha}+k^\rho k^\alpha$ is the inverse propagator.

In Eq. (5), $F_i(q^2)$ are related to the charge, magnetic, and quadrupole e.m. FFs of the deuteron (see, e.g., [25]):

$$G_C(q^2)=F_1(q^2)+\frac{2}{3}\eta G_Q(q^2),$$

$$G_M(q^2)=F_2(q^2),$$

$$G_Q(q^2)=F_1(q^2)-F_2(q^2)+(1+\eta)F_3(q^2),$$

$$\eta=-\frac{q^2}{4m_2^2}. \tag{7}$$

B. Internal radiation amplitude

Apart from the external amplitude there are other more complicated processes, such as initial-state *pd* rescattering and MEC. This contribution (henceforth called the internal amplitude $M_{\rm int}$) can be constrained by imposing the gauge invariance requirement for the total amplitude $M=M_{\rm ext}+M_{\rm int}$.

Contracting $M_{\rm ext}$ with the photon momentum and imposing gauge invariance for the total amplitude leads to the following condition:

$$q_\mu M_{\rm int}^{\mu\alpha}=-q_\mu M_{\rm ext}^{\mu\alpha}=\Phi^\alpha(p_3,p_2,p_1-q)+\Phi^\alpha(p_3,p_2-q,p_1)-2\Phi^\alpha(p_3+q,p_2,p_1). \tag{8}$$

So far we have not specified the form of the pd^3He vertex function. For the case where at most one particle is off its mass shell it has the following general structure:

$$\Phi^\alpha(k_3,k_2,k_1)=\phi_+^\alpha(k_3,k_2,k_1)+\phi_{-,p}^\alpha(k_3,k_2,k_1)\frac{\not k_1-m_1}{2m_1}+\frac{\not k_3-m_3}{2m_3}\phi_{-,h}^\alpha(k_3,k_2,k_1), \tag{9}$$

where the last two terms contribute when the proton or helion are off their mass shells, and momentum conservation implies $k_3=k_1+k_2$. The Dirac structure of ϕ_+^α can be written as

$$\phi_+^\alpha(k_3,k_2,k_1)=(\gamma^\alpha G_+-k_1^\alpha H_{1+}-k_2^\alpha H_{2+})\gamma_5, \tag{10}$$

and $\phi_{-,p}^\alpha$ and $\phi_{-,h}^\alpha$ are expressed similarly in terms of $G_{-,p},H_{1-,p},H_{2-,p}$ and $G_{-,h},H_{1-,h},H_{2-,h}$, respectively.

In the following we will use a more restricted form [16], in which the vertex is expressed only through the relative *pd* four-momentum $Q^\alpha=(M_r/m_1)k_1^\alpha-(M_r/m_2)k_2^\alpha$ [where $M_r=m_1m_2/(m_1+m_2)$ is the reduced mass of the *pd* system]. The vertex then becomes

$$\phi_+^\alpha(k_3,k_2,k_1)=[\gamma^\alpha G_+(Q^2)-Q^\alpha H_+(Q^2)]\gamma_5,$$

$$\phi_{-,p}^\alpha(k_3,k_2,k_1)=\phi_{-,h}^\alpha(k_3,k_2,k_1)=\phi_-^\alpha(k_3,k_2,k_1)=[\gamma^\alpha G_-(Q^2)-Q^\alpha H_-(Q^2)]\gamma_5, \tag{11}$$

where $G_+(Q^2)$ and $H_+(Q^2)$ can be directly related with the nonrelativistic WF. For the ^{3}He, proton, and deuteron diagrams in Fig. 1 the relative momenta take the values $Q_3^\alpha=(M_r/m_1)p_1^\alpha-(M_r/m_2)p_2^\alpha$, $Q_1^\alpha=Q_3^\alpha-(M_r/m_1)q^\alpha$, and $Q_2^\alpha=Q_3^\alpha+(M_r/m_2)q^\alpha$, respectively.

Using the structure of this vertex and the Dirac equation for initial and final spinors one obtains, from Eq. (8)

$$q_\mu M_{\rm int}^{\mu\alpha}=\left\{[\gamma^\alpha G_-(Q_1^2)-Q_1^\alpha H_-(Q_1^2)]\frac{\not q}{2m_1}-\frac{\not q}{m_3}[\gamma^\alpha G_-(Q_3^2)-Q_3^\alpha H_-(Q_3^2)]+q^\alpha\left[\frac{M_r}{m_1}H_+(Q_1^2)-\frac{M_r}{m_2}H_+(Q_2^2)\right]\right.$$
$$\left.+\gamma^\alpha[G_+(Q_1^2)+G_+(Q_2^2)-2G_+(Q_3^2)]-Q_3^\alpha[H_+(Q_1^2)+H_+(Q_2^2)-2H_+(Q_3^2)]\right\}\gamma_5. \tag{12}$$

Now one can write an finite-difference identity for the combination appearing on the right-hand side of Eq. (12),

$$G_+(Q_1^2)+G_+(Q_2^2)-2G_+(Q_3^2)=G_+'(Q_1^2)(Q_1^2-Q_0^2)+G_+'(Q_2^2)(Q_2^2-Q_0^2)-2G_+'(Q_3^2)(Q_3^2-Q_0^2), \tag{13}$$

$$G_+'(Q_i^2)=[G_+(Q_i^2)-G_+(Q_0^2)]/(Q_i^2-Q_0^2), \tag{14}$$

where $i=1,2,3$ and the four-momentum Q_0, used as the expansion point, is in principle arbitrary.

If we choose $Q_0^2=Q_3^2$, then from Eqs. (12) and (13) it follows that a solution for the internal amplitude can be constructed as $M_{\rm int}^{\mu\alpha}=M_{\rm int}^{\mu\alpha}(1)+M_{\rm int}^{\mu\alpha}(2)$, i.e.,

$$M_{\rm int}^{\mu\alpha}(1)=\left\{[\gamma^\alpha G_-(Q_1^2)-Q_1^\alpha H_-(Q_1^2)]\frac{\gamma^\mu}{2m_1}-\frac{\gamma^\mu}{m_3}[\gamma^\alpha G_-(Q_3^2)-Q_3^\alpha H_-(Q_3^2)]\right\}\gamma_5+g^{\mu\alpha}\left[\frac{M_r}{m_1}H_+(Q_1^2)-\frac{M_r}{m_2}H_+(Q_2^2)\right]\gamma_5, \quad (15)$$

$$M_{\rm int}^{\mu\alpha}(2)=\frac{M_r}{m_1}(q-2p_1)^\mu R_1^\alpha+\frac{M_r}{m_2}(q-2p_2)^\mu R_2^\alpha+\frac{M_r}{m_1+m_2}(q+2p_3)^\mu(R_1^\alpha+R_2^\alpha), \quad (16)$$

where we used the notation $R_i^\alpha=[\gamma^\alpha G'_+(Q_i^2)-Q_3^\alpha H'_+(Q_i^2)]\gamma_5$ (for $i=1,2$), and $H'_+(Q_i^2)$ is defined similarly to Eq. (14). In deriving Eq. (16) the relations

$$Q_1^2=\Delta+\frac{M_r}{m_1}q\cdot(q-2p_1),\quad Q_2^2=\Delta+\frac{M_r}{m_2}q\cdot(q-2p_2),$$

$$Q_3^2=\Delta-\frac{M_r}{m_1+m_2}q\cdot(q+2p_3) \quad (17)$$

have also been used, where

$$\Delta=M_r(m_1+m_2-m_3)\left(1+\frac{m_3}{m_1+m_2}\right)\approx 2M_r(|\varepsilon_h|-|\varepsilon_d|) \quad (18)$$

accounts for the difference between the binding energies of the deuteron and ^{3}He. Note that the amplitude in Eq. (16) remains finite in the special case when $Q_1^2\to Q_3^2$ or $Q_2^2\to Q_3^2$.

Of course one could choose, instead of $Q_0^2=Q_3^2$ in Eq. (16), $Q_0^2=Q_1^2$, or $Q_0^2=Q_2^2$, or an ''averaged'' momentum

$$Q_0^2=x_1Q_1^2+x_2Q_2^2+x_3Q_3^2, \quad (19)$$

with parameters x_i, independent of q^μ, satisfying the condition $x_1+x_2+x_3=1$. For *real* photons all choices lead to the same transition amplitude.

To verify this we apply again Eq. (13) for the average Q_0^2 (and similar equation for H_+) in Eq. (12) and find the amplitude $M_{\rm int}(2)$ in a different form (marked by ''tilde'')

$$\tilde{M}_{\rm int}^{\mu\alpha}(2)=\frac{M_r}{m_1}(q-2p_1)^\mu[(x_2+x_3)R_1^\alpha-x_1R_2^\alpha+2x_1R_3^\alpha]+\frac{M_r}{m_2}(q-2p_2)^\mu[(x_1+x_3)R_2^\alpha-x_2R_1^\alpha+2x_2R_3^\alpha]+\frac{M_r}{m_1+m_2}(q+2p_3)^\mu\times[2(x_1+x_2)R_3^\alpha+x_3R_1^\alpha+x_3R_2^\alpha]. \quad (20)$$

This reduces to Eq. (16) if $x_1=x_2=0$ and $x_3=1$.

Using Eq. (19), and a relation $m_1Q_1^2+m_2Q_2^2-(m_1+m_2)Q_3^2=M_rq^2$ which follows from Eq. (17) and energy-momentum conservation, one obtains

$$Q_1^2-Q_0^2=-2q\cdot Q_3\left[\frac{M_r}{m_1}(1-x_1)+\frac{M_r}{m_2}x_2\right],$$

$$Q_2^2-Q_0^2=2q\cdot Q_3\left[\frac{M_r}{m_2}(1-x_2)+\frac{M_r}{m_1}x_1\right],$$

$$Q_3^2-Q_0^2=2q\cdot Q_3\left(\frac{M_r}{m_1}x_1-\frac{M_r}{m_2}x_2\right). \quad (21)$$

Finally we consider the contraction of $\tilde{M}_{\rm int}(2)$ with the photon polarization vector. As a result of the condition $q\cdot\epsilon=0$, the momentum p_3^μ can be replaced by $p_1^\mu+p_2^\mu$ in Eq. (20). Then the four-momentum in front of R_1^α reduces to

$$-2Q_3^\mu\left[\frac{M_r}{m_1}(1-x_1)+\frac{M_r}{m_2}x_2\right], \quad (22)$$

and comparing this expression with the first relation in Eq. (21) one observes that the factor in square brackets involving x_1 and x_2 cancels in the amplitude Eq. (20) with the similar factor in the definition of R_1^α. Similar cancellations occur in the terms related to R_2^α and R_3^α. Also $G_+(Q_0^2)$ and $H_+(Q_0^2)$ drop out due to a cancellation between the three different contributions and one arrives at

$$\epsilon_\mu\tilde{M}_{\rm int}^{\mu\alpha}(2)=\frac{Q_3\cdot\epsilon}{Q_3\cdot q}\{\gamma^\alpha[G_+(Q_1^2)+G_+(Q_2^2)-2G_+(Q_3^2)]-Q_3^\alpha[H_+(Q_1^2)+H_+(Q_2^2)-2H_+(Q_3^2)]\}\gamma_5. \quad (23)$$

The seeming singularity at $Q_3\cdot q=0$ is fictitious because any difference $Q_i^2-Q_j^2$ $(i\neq j=1,2,3)$ is proportional to $Q_3\cdot q$ [as can be seen from Eq. (21)].

This expression does not depend on x_i and on Q_0^2, which is what we set out to prove. Although Eq. (20) looks different from Eq. (16), they give identical results when contracted with ϵ_μ.

In the case of the *virtual* photons Eq. (20) does not lead to Eq. (23), and Eq. (16) and Eq. (20) give different results. A convenient choice for the average momentum in this case is $Q_0^2=Q_3^2$ because this variable is a function of only the invariant energy $s=m_3^2+q\cdot(q+2p_3)$ (or the incoming proton energy) and does not depend on the scattering angle [see Eq. (17)].

It is of interest to consider the limit of small photon energies. From Eq. (17) it is seen that for $q\to 0$ one has $Q_1^2=Q_2^2=Q_3^2\to\Delta$. The finite differences introduced in Eq. (14) then reduce to the derivative $G'_+(Q_i^2)=dG_+(Q^2)/dQ^2|_{Q^2=\Delta}$. This case would correspond to the situation where all particles in the pd^3He vertex are on their mass shells. Although this is excluded because of energy-momentum conservation, this limit may be used for deriving a soft-photon approximation [15] for real photons. To obtain the soft-photon amplitude one has to expand $G_+(Q_i^2)$ and

$H_+(Q_i^2)$ around Δ and keep terms of order q^{-1} and q^0 in $M_{\rm ext}$ and terms of order q^0 in $M_{\rm int}$. As a check of our results we verified that $M=M_{\rm ext}+M_{\rm int}$ reproduces the amplitude of [15] when $q\to 0$.

One consequence of the internal amplitude derived above is a cancellation of the terms proportional to the ''negative-energy'' components ϕ_-^α with the corresponding terms in the external amplitude which are related to the γ^μ part of the e.m. vertex. For the proton amplitude we have, e.g.,

$$\phi_-^\alpha(p_3,p_2,p_1-q)\frac{\not p_1-\not q-m_1}{2m_1}S(p_1-q,m_1)\gamma^\mu = \phi_-^\alpha(p_3,p_2,p_1-q)\frac{\gamma^\mu}{2m_1}. \quad (24)$$

This term exactly cancels the first term in Eq. (15). A similar cancellation occurs between the second term in Eq. (15) and the ϕ_-^α contribution from the ^{3}He diagram. As a result, the ϕ_-^α terms contribute only to the part of the amplitude related to the anomalous magnetic moments of the proton and helion. In fact, this cancellation is not very surprising if one recalls the derivation of the LET for bremsstrahlung [13] (see also [26]). There negative-energy contributions due to gauge invariance also did not contribute in the leading orders q^{-1} and q^0, and appeared in the amplitude only in higher orders.

It is seen from the structure of $M_{\rm int}$ that it can be combined with the external amplitude into a sum of ''effective'' proton, deuteron, and ^{3}He terms: $M=M_{\rm ext}+M_{\rm int}\equiv A_1+A_2+A_3$, where each amplitude A_i is gauge invariant by itself, i.e., $q_\mu A_1^{\mu\alpha}=q_\mu A_2^{\mu\alpha}=q_\mu A_3^{\mu\alpha}=0$. Expressions for A_i are given in Appendix B. Note that we checked explicitly the fulfillment of gauge invariance in the numerical calculations.

Of course we realize that the above construction of the internal amplitude is not unique, and terms which are gauge invariant themselves and vanish in the limit $q\to 0$ may be added to $M_{\rm int}$. In the method outlined above one particular ambiguity stems from the choice of the reference point Q_0^2. A possible choice is $Q_0^2=\Delta$, which cannot be cast in the form of Eq. (19) with constant parameters x_i. This results in a different amplitude $M_{\rm int}(2)$ (denoted below by a caret):

$$\hat M_{\rm int}^{\mu\alpha}(2)=\frac{M_r}{m_1}(q-2p_1)^\mu\hat R_1^\alpha+\frac{M_r}{m_2}(q-2p_2)^\mu\hat R_2^\alpha + \frac{2M_r}{m_1+m_2}(q+2p_3)^\mu\hat R_3^\alpha, \quad (25)$$

where

$$\hat R_i^\alpha=[\gamma^\alpha\hat G'_+(Q_i^2)-Q_3^\alpha\hat H'_+(Q_i^2)]\gamma_5,$$
$$\hat G'_+(Q_i^2)=[G_+(Q_i^2)-G_+(\Delta)]/(Q_i^2-\Delta). \quad (26)$$

The cross sections for this amplitude, however, prove unsatisfactory (factor of 30 too large) when compared with capture data at energies about 200 MeV. The reason is the following: the functions $G_+(Q_i^2)$ and $H_+(Q_i^2)$ are rapidly varying when going from the point $Q^2=\Delta>0$ to the values Q_i^2 which are negative in the physical region. The finite differences in Eq. (26) then become very large and the choice $Q_0^2=\Delta$ would be the most unfortunate. Only in the limit of $q\to 0$ does Eq. (25) become equivalent to Eq. (16) and both amplitudes converge to the LET. This implies that the amplitudes in Eq. (16) and Eq. (25) coincide in the leading order of q^0, but differ in higher orders.

In the calculation we include the dominant components [17–19] of the ^{3}He WF, i.e. a *pn* pair in the deuteron state or in the $^1S_0$ (quasi) bound d^* state, coupled to a proton. The $pd\to pd^*$ capture mechanism via the spin-flip $^3S_1+{}^3D_1\to{}^1S_0$ transition has been shown [16] to be important and is therefore included explicitly. The corresponding amplitude (see Fig. 1, last graph) can be written as

$$M_{d*}^{\mu\alpha}=\Theta(p_3,p_2-q,p_1)\Delta(p_2-q)\Gamma^{\mu\alpha}(p_2-q,p_2), \quad (27)$$

where $\Delta(k)=(k^2-m_2^{*2}+i0)^{-1}$ and the e.m. vertex has the form

$$\Gamma^{\mu\alpha}(p_2-q,p_2)=-\frac{i}{m_1}\mu_v\varepsilon^{\mu\alpha\rho\nu}q_\rho(p_2)_\nu F(q^2). \quad (28)$$

Here $\mu_v=\mu_p-\mu_n$ is the isovector magnetic moment of the nucleon, m_2^* is the mass of the d^*, $F(q^2)$ is the transition form factor, and $\Theta(p_3,p_2-q,p_1)$ is the $pd^*{}^3$He vertex function. This contribution is gauge invariant by itself, and does not affect the above discussion on the internal amplitude.

C. ^{3}He vertex function

In order to relate the invariant functions $G_\pm(Q^2),H_\pm(Q^2)$ to the overlap integral $\langle d|{}^3\mathrm{He}\rangle$ we recall that the latter is written as [19]

$$\psi_{pd}(\vec r)=\sum_{LM_LSM_S}C^{1/2m_h}_{LM_LSM_S}C^{SM_S}_{1m_d1/2m_p}R_L(r)Y_{LM_L}(\hat r) \quad (r=|\vec r|,\ \hat r=\vec r/r), \quad (29)$$

where $\vec r$ is the relative *pd* coordinate, $R_0(r)[R_2(r)]$ is the $S[D]$ radial WF corresponding to the total spin $\frac{1}{2}[\frac{3}{2}]$, and m_h, m_d, and m_p are the spin projections for helion, deuteron, and proton, respectively.

In momentum space this WF can be represented in the form

$$\psi_{pd}(\vec p)=-\frac{1}{\sqrt{3}}\chi^*_{m_h}\left\{u(p)\vec\sigma\vec\xi(m_d) - \frac{1}{\sqrt{2}}v(p)[3\vec\sigma\hat p\vec\xi(m_d)\hat p-\vec\sigma\vec\xi(m_d)]\right\} \times Y_{00}(\hat p)\chi_{m_p}, \quad (30)$$

where $\vec\xi(m_d)$ are the deuteron polarization vectors [Appendix C, Eq. (C8)], $u(p)=R_0(p)$, $v(p)=R_2(p)$, and

$$R_L(p)=i^L\sqrt{\frac{2}{\pi}}\int_0^\infty j_L(pr)R_L(r)r^2dr. \tag{31}$$

The relation between $G_\pm(Q^2),H_\pm(Q^2)$ in Eq. (10) and components u,v reads [16] as

$$G_+(Q^2)=N\left[u(|\vec{Q}|)+\frac{1}{\sqrt{2}}\frac{\vec{Q}^2}{\alpha^2}v(|\vec{Q}|)\right](\vec{Q}^2+\alpha^2),$$

$$H_+(Q^2)=\frac{1}{m_2}N\left[u(|\vec{Q}|)+\frac{1}{\sqrt{2}}\frac{\vec{Q}^2}{\alpha^2}\left(1+\frac{6m_1m_2}{\vec{Q}^2}\right)v(|\vec{Q}|)\right]\times(\vec{Q}^2+\alpha^2),$$

$$G_-(Q^2)=N\frac{1}{\sqrt{2}}\frac{\vec{Q}^2}{\alpha^2}v(|\vec{Q}|)(\vec{Q}^2+\alpha^2),$$

$$H_-(Q^2)=\frac{1}{m_2}N\frac{1}{\sqrt{2}}\frac{\vec{Q}^2}{\alpha^2}\left(1+\frac{6m_1m_2}{\vec{Q}^2}\right)v(|\vec{Q}|)(\vec{Q}^2+\alpha^2), \tag{32}$$

with the normalization constant $N=\pi\sqrt{m_3/(6m_1M_r)}$ and $\alpha=\sqrt{2M_r(m_1+m_2-m_3)}\approx\sqrt{\Delta}$.

This relation has been obtained in [16] in the nonrelativistic limit following the formalism developed previously for the deuteron [27] (see also [28]). Strictly speaking, the functions G_- and H_- cannot be obtained unambiguously from the nonrelativistic WF of ^{3}He. In particular, the last two equations in Eqs. (32) are based on certain assumptions about the negative energy part of the fermion propagators at low energies.

The $pd^*{}^3$He vertex $\Theta(p_3,p_2-q,p_1)=I(Q_2^{*2})$ is related [16] to the overlap integral $\psi_{pd*}(\vec{p})=\langle d^*|^3\mathrm{He}\rangle$:

$$\psi_{pd*}(\vec{p})=\frac{1}{\sqrt{3}}\chi^*_{m_h}w(p)\,Y_{00}(\hat{p})\chi_{m_p},$$

$$I(Q^2)=\pi\sqrt{m_3/(6m_1M_r^*)}w(|\vec{Q}|)(\vec{Q}^2+\alpha^{*2}), \tag{33}$$

where the variables Q_2^*, M_r^*, and α^* can be obtained from, respectively, Q_2, M_r, and α for the deuteron amplitude by changing m_2 to m_2^*.

The effective number of pd pairs and pd^* pairs is given, respectively, by the integrals

$$N_{pd}=\int_0^\infty[|u(p)|^2+|v(p)|^2]p^2dp,$$

$$N_{pd*}=\int_0^\infty|w(p)|^2p^2dp. \tag{34}$$

Two models for the ^{3}He WF have been used in calculations. The first model (called model ''a'') is a recent calculation [19] with the Argonne v18 NN+Urbana IX $3N$ interaction. This calculation yields $N_{pd}=1.33$ and $N_{pd*}=1.28$. Here the (quasibound) d^* WF was replaced by a bound WF by multiplying the NN potential in the $^1S_0$ channel by a factor which was determined so as to make the normalization of the overlap function $\langle d^*|^3\mathrm{He}\rangle$ maximal. The sum $N_{pd}+N_{pd*}=2.61$ gives the bulk of the normalization but does not exhaust it.

The second one (called model ''b'') is the parametrization in [16], which was based on calculations in Ref. [17] with the Argonne v14 NN+Urbana VII $3N$ interaction. In the model [16] the pd and pd^* pairs are assumed to occur in ^{3}He with equal probability, and together to saturate the normalization integral, i.e., $N_{pd}=N_{pd*}=3/2$.

D. Electromagnetic form factors

In order to calculate the e.m. FFs of the proton we used the extended vector meson dominance model [29]. The deuteron FFs were taken from the calculation in [18] with Argonne NN interaction (including $3N$ forces, MEC and relativistic corrections) and we used the parametrization of the FFs of the ^{3}He as given in [30]. For the FF of the transition $d\to{}^1S_0$ we used an approximation consistent with treating $^1S_0$ as a quasibound state. The FF is calculated as the deuteron electric FF with only the S component of the WF (model from [31] has been used). The reason is that the q^2 dependence of the threshold deuteron electrodisintegration is known to be strongly influenced by the MEC. At the same time at the relatively small $|q^2|<0.15$ GeV^2 the effect of the MEC is opposite to that of the D wave in the deuteron [32], and the q^2 dependence is approximately governed by the S component.

At the real photon point the FFs are normalized to

$$F_1^p(0)=F_1^h(0)=G_C(0)=1,\quad F_2^p(0)=\mu_p-1,$$

$$F_2^h(0)=\frac{m_3}{m_1}\mu_h-2,\quad G_M(0)=\frac{m_2}{m_1}\mu_d,\quad G_Q(0)=m_2^2Q_d, \tag{35}$$

where $Q_d=0.2859$ fm^2 is the quadrupole moment of the deuteron and the magnetic moments of the proton, deuteron, and ^{3}He (in nuclear magnetons) are $\mu_p=2.7928$, $\mu_d=0.85774$, and $\mu_h=-2.12755$, respectively.

III. ADDITIONAL EFFECTS IN THE ^{3}He CONTRIBUTION

So far the propagators for the proton, deuteron, and helion were taken as the propagators of elementary spin-1/2 and spin-1 fields. For composite objects this may be a poor approximation and in this section we investigate the effects of possible modifications. These may occur because of the internal structure, which is manifested in possible resonances and decay modes. One can expect these effects to be most important for propagation in the continuum where the invariant mass W is larger than the mass of the free particle; therefore we will focus on the ^{3}He contribution for which $W_3=\sqrt{s}>m_3$.

A. ^{3}He self-energy

The modification of the propagator $S(p)$ for a spin-$\frac{1}{2}$ particle with mass m is most easily discussed in terms of the self-energy $\Sigma(p)$, in terms of which $S(p)=[\not{p}-m+\Sigma(p)]^{-1}$. The self-energy can be written as $\Sigma(p)$

$=A(p^2)\not{p}+B(p^2)m$, with (complex) scalar functions $A(p^2)$ and $B(p^2)$ that must satisfy the conditions

$$A(m^2)+B(m^2)=A(m^2)+2m^2[A'(m^2)+B'(m^2)]=0, \tag{36}$$

in order to leave the pole position (at the physical mass m) and the residue at the pole unchanged. The prime above stands for the derivative d/dp^2.

If we make the assumption that $A(p^2)=-B(p^2)$, where $A(p^2)$ vanishes at $p^2=m^2$, then the conditions of Eq. (36) are automatically fullfilled. In this case the propagator becomes

$$S(p)=[1+\alpha(p^2)]\frac{\not{p}+m}{p^2-m^2}, \tag{37}$$

where we have introduced a parameter $\alpha(p^2)=[1+A(p^2)]^{-1}-1$, which vanishes at $p^2=m^2$. We will treat $\alpha(p^2)$ as an adjustable phenomenological parameter in the ^{3}He self-energy when comparing calculations with the experimental data in Sec. IV.

Intimately related to the self-energy are the so-called off-shell effects in the e.m. vertex. In constructing the vertex care should be taken of the WT identity $q\cdot\Gamma(p+q,p)=Z[S^{-1}(p+q)-S^{-1}(p)]$ ($Z=2$ is the charge of the ^{3}He). For initial on-mass-shell and final off-shell states the e.m. vertex can be written as

$$\Gamma^\mu(p',p)u(p)=\left\{Z\gamma^\mu[1+\alpha(p'^2)]^{-1}+i\frac{\kappa}{2m}\sigma^{\mu\nu}q_\nu\right\}u(p) \tag{38}$$

for a real photon with momentum q and $p'=p+q$. It should be noted that since the magnetic contribution is not fixed by the WT identity, this construction of the vertex is not unique. We have opted for a choice which is most convenient for our application where only the convection current part of the vertex is modified.

The contraction of the e.m. vertex with the propagator leads to

$$\begin{aligned}S(p')\Gamma^\mu(p',p)u(p)&=\frac{Z(p+p')^\mu}{p'^2-m^2}u(p)+\frac{1}{p'^2-m^2}\\&\times\left[Z+[1+\alpha(p'^2)]\frac{\not{p}'+m}{2m}\kappa\right]i\sigma^{\mu\nu}q_\nu u(p).\end{aligned} \tag{39}$$

The first term on the right-hand side is the same as one would obtain with the unmodified propagator and vertex. It thus appears that $\Sigma(p)$ modifies only the anomalous magnetic moment κ, which is replaced by $\kappa_{\rm eff}=\kappa[1+\alpha(p^2)]$. In general, for any e.m. vertex satisfying the WT identity only the magnetic part of the product $S(p')\Gamma^\mu(p',p)u(p)$ gets modified. One gets a similar expression for the initial off-shell and final on-shell states. These results can easily be generalized for virtual photons.

Note that the construction of the internal amplitude for the $p+d\to{}^3\mathrm{He}+\gamma^*$ reaction in Sec. II B remains unchanged and independent of $\alpha(p^2)$.

B. Effect of *pd* rescattering

Another aspect to include is the effect of the initial-state *pd* rescattering. In the channel with quantum numbers $J^P=\frac{1}{2}^+$ the latter can be approximately taken into account by modifying the pd^3He vertex Φ to

$$\Psi_{lS}(|\vec{Q}|,E)=[1+iT_{lS}(E)]\Phi_{lS}(|\vec{Q}|)\approx\sqrt{S_{lS}(E)}\Phi_{lS}(|\vec{Q}|), \tag{40}$$

where l is the angular momentum, S is the total proton-deuteron spin, and where the partial T matrix is defined in terms of the *pd* scattering phase shift $\delta_{lS}(E)$ and the inelasticity parameter $\eta_{lS}(E)$ via the S matrix $S_{lS}(E)=\eta_{lS}(E)e^{2i\delta_{lS}(E)}=1+2iT_{lS}(E)$ [6]. This creates a complex function with a phase related to the *pd* phase shift, as should be expected from unitarity arguments [33].

This procedure can be justified by considering a separable model for the *pd* T matrix. When constructing the amplitude for the diagram of Fig. 1 where the photon is radiated from the ^{3}He, it was implied that the T matrix was approximated by the pole contribution from the ^{3}He bound state only:

$$\begin{aligned}T^{\alpha\beta}(Q,Q';P)&\approx V_B^{\alpha\beta}(Q,Q';P)\\&=\bar{\Phi}^\alpha(Q)(\not{P}-m_3)^{-1}\Phi^\beta(Q'),\end{aligned} \tag{41}$$

where $P=(\sqrt{s},\vec{0})$, $\bar{\Phi}^\alpha(Q)=\gamma_0\Phi^\alpha(Q)^\dagger\gamma_0$ is the $^3\mathrm{He}\to pd$ vertex. The pole contribution is expressed through the vertex $\Phi^\alpha(Q)\equiv\Phi^\alpha(Q;s=m_3^2)$ which is a real function dependent on the relative *pd* momentum Q.

We will treat now $V_B(E)$ as the interaction kernel in the Bethe-Salpeter equation for the *pd* system:

$$\tilde{T}(E)=V_B(E)+\frac{i}{(2\pi)^4}V_B(E)\otimes G(E)\otimes\tilde{T}(E), \tag{42}$$

where $E=\sqrt{s}-m_3$ is the excitation energy or ''off-shellness'' of the helion, the integration over the intermediate relative momentum is implied, deuteron tensor indices are supressed, and $G(E)$ is the product of the free proton and deuteron propagators.

The separable form for $V_B(E)$ results in a separable solution for $\tilde{T}$:

$$\tilde{T}^{\alpha\beta}(Q,Q';P)=\bar{\Phi}^\alpha(Q)(\not{P}-m_3)^{-1}\Psi^\beta(Q';E), \tag{43}$$

where

$$\Psi(E)=\Phi+\frac{i}{(2\pi)^4}\Phi\otimes G(E)\otimes\tilde{T}(E). \tag{44}$$

This generates a complex-valued vertex $\Psi^\alpha(Q;E)$ which in addition contains a dependence on the invariant mass of the intermediate ^{3}He and reduces to $\Phi^\alpha(Q)$ at zero energy. To relate $\Psi(E)$ to the on-shell T matrix we pick out the contribution to the integral in Eq. (44) coming from the pole

part of the propagator $G(E)$. After applying Cutkosky's rules and partial wave decomposition one then obtains Eq. (40). Now we identify $\tilde{T}$ with the measured on-shell T matrix which is expressed through the *pd* scattering phase shifts and inelasticity parameters.

In implementing this in the calculation of the photon radiative amplitude care should be taken of the counter terms (or the internal amplitude) introduced to obey gauge invariance (see Sec. II B). Since there is no unique procedure to follow, we have opted for one particular choice. Part of the contributions from the proton and deuteron diagrams of Fig. 1 (for which the excitation energy $E_1=E_2=0$) are current conserving by themselves. For these magnetic terms the original real vertex $\Phi^\alpha(Q)$ is used. For the corresponding contribution from the helion diagram in Fig. 1 (where the excitation energy $E_3\approx 2/3T_p$ is positive and large), we use the modified $\Psi^\alpha(Q_3;E_3)$ instead of $\Phi^\alpha(Q_3)$.

Gauge invariance closely relates the convection-current contribution from the different external radiation diagrams with the internal one. For this reason we use the modified vertex $\Psi^\alpha(Q;E_3)$ in all of these terms. These contributions to the amplitude combined can be put in the form

$$\Psi^\alpha(Q_1;E_3)\left[\frac{(2p_1-q)^\mu}{D_1}-\frac{M_r}{m_1}\frac{\left(2Q_3-\frac{M_r}{m_1}q\right)^\mu}{Q_1^2-Q_3^2}\right] \tag{45}$$

$$+\Psi^\alpha(Q_2;E_3)\left[\frac{(2p_2-q)^\mu}{D_2}+\frac{M_r}{m_2}\frac{\left(2Q_3+\frac{M_r}{m_2}q\right)^\mu}{Q_2^2-Q_3^2}\right] \tag{46}$$

$$+\Psi^\alpha(Q_3;E_3)\left[2\frac{(2p_3+q)^\mu}{D_3}+\frac{M_r}{m_1}\frac{\left(2Q_3-\frac{M_r}{m_1}q\right)^\mu}{Q_1^2-Q_3^2}-\frac{M_r}{m_2}\frac{\left(2Q_3+\frac{M_r}{m_2}q\right)^\mu}{Q_2^2-Q_3^2}\right], \tag{47}$$

which closely resembles the equivalent terms in Eqs. (B4), (B5), and (B7) of Appendix B.

In order to have an idea of the effect of *pd* rescattering on other partial waves, we included the intermediate $\frac{3}{2}^-$ resonance, $R_{3/2^-}$, situated at 14 MeV excitation energy and with a decay width of 10 MeV. This resonancelike structure has been observed in the *pd* phase shift analysis [34] and in other reactions (see [35] and references therein). For the $pd\to R_{3/2^-}$ and $R_{3/2^-}\to\gamma^3$He vertices the following couplings have been used, respectively:

$$\Phi^{\rho\alpha}(p_3+q,p_2,p_1)=-\frac{i}{2m_3}G_1(s)(\not{p}_2 g^{\rho\alpha}-p_2^\rho\gamma^\alpha)\gamma_5,$$

$$\Gamma^{\mu\beta}(p_3,p_3+q)=-\frac{i}{2m_3}G_2(s)(\not{q}g^{\mu\beta}-q^\beta\gamma^\mu). \tag{48}$$

The corresponding amplitude can be written as

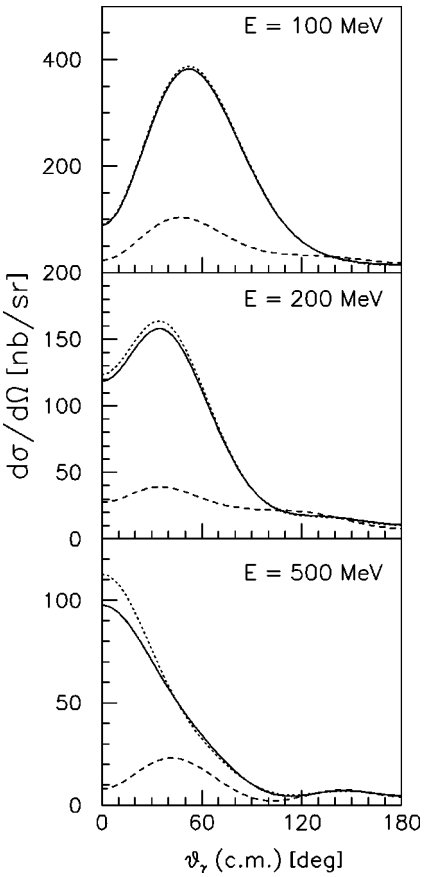

FIG. 2. Cross sections for the $pd\to{}^3\mathrm{He}\gamma$ reaction at proton laboratory energies 100, 200, and 500 MeV, calculated with the wave function [19]. Solid lines, default calculations; dotted lines, calculations without the negative-energy components G_-, H_- in the pd^3He vertex; and dashed lines, calculations without the internal amplitude.

$$M_R^{\mu\alpha}=\Gamma^{\mu\beta}(p_3,p_3+q)S_{\beta\rho}(p_3+q)\Phi^{\rho\alpha}(p_3+q,p_2,p_1), \tag{49}$$

where $S_{\beta\rho}(p_3+q)$ is the Rarita-Schwinger propagator including the decay width.

For many observables the inclusion of *pd* rescattering is only of secondary importance. It is crucial, however, for the vector analyzing power A_y. Since the corresponding spin-density matrix is imaginary, nonvanishing values for A_y are obtained only if the matrix elements have nontrivial complex phases. As a result of the low excitatation energy of the $\frac{3}{2}^-$ resonance, it has a sizable effect on A_y and some other spin observables in *pd* capture at small energies in the range of about 5–20 MeV. At higher energies it has a small effect.

IV. RESULTS OF CALCULATIONS AND DISCUSSION

Before comparing to the experimental data, we first study in Fig. 2 the importance of some of the ingredients of the model to the $pd\to\gamma^3$He cross sections at energies above 100 MeV. First, one notices that the internal amplitude M_{int} has a substantial effect at angles less then 120°. As a result, the calculation including only the external radiation (dashed lines) would strongly underestimate the data (shown in Fig. 3 and Fig. 4). The calculations are performed in the Coulomb

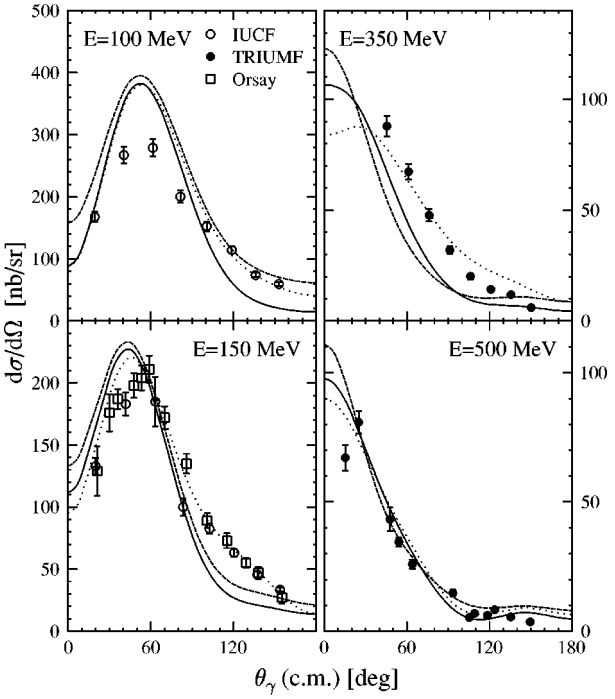

FIG. 3. Cross sections for the $pd \rightarrow {}^3\mathrm{He}\gamma$ reaction at proton laboratory energies 100, 150, 350, and 500 MeV. The points are from [38], [39], and [1]. Solid lines are the default calculations for the wave function [19]. Dotted lines show the effect of the ^{3}He self-energy, and dashed lines are calculations including *pd* scattering phase shifts.

gauge; of course only the total amplitude including M_{int} is independent of the photon gauge. The large contribution of the internal amplitude persists at small energies down to $\approx$10 MeV. This goes in line with nonrelativistic calculations, where the MECs have been shown to be important at small energies (see, e.g. [9]). Note that the large effect of the internal contribution for the electron asymmetry in the $^3\mathrm{He}(e,e'p)d$ reaction had been noticed earlier in [40]. Second, the contribution of the negative-energy components G_- and H_- in the pd^3He vertex turns out to be small. This can be explained by the partial cancellation of these terms in the external and internal amplitude, as was mentioned in Sec. II B. The effect of G_- and H_- increases with energy as expected, though we do not ascribe too much significance to this as the pd^3He vertex was calculated on the basis of a nonrelativistic ^{3}He WF.

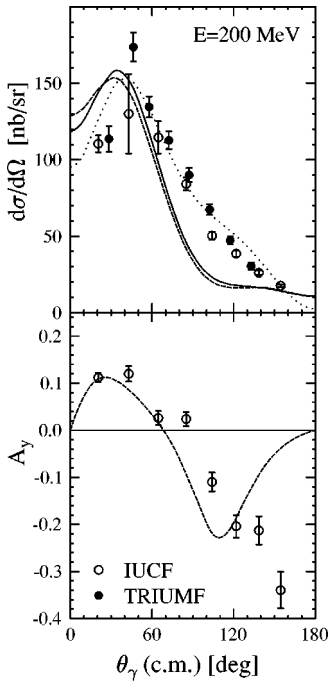

FIG. 4. Cross section and analyzing power A_y for proton laboratory energy 200 MeV. Notation for the curves is the same as in Fig. 3.

TABLE I. Values used for the parameter $\alpha(p^2)$ (see Sec. III A). T_p^{lab} is quoted for proton capture on the deuteron.

T_p^{lab} [MeV]	T_{pd}^{cm} [MeV]	E_γ^{cm} [MeV]	α
100	65.9	70	1.0
150	98.3	102	1.3
200	130.3	133	1.4
300	193.3	192	1.2
350	224.4	221	1.0
400	255.0	249	0.7
450	285.5	277	0.5
500	315.6	305	0.3

In Appendix C we collected definitions of the various observables which are discussed in this section. We will refer to calculations based on the expressions in Sec. II as ''default.'' Apart from this we will also present results obtained either by including the self-energy correction (Sec. III A) or by including the phase shifts (Sec. III B), and compare them to the experimental data.

Figures 3 and 4 show the angular distributions and the proton analyzing power for the $pd \rightarrow \gamma^3$He at the proton laboratory energy T_p in the interval 100–500 MeV. The default calculation is in qualitative agreement with experiment. However, at energies less than 350 MeV it underpredicts the cross sections at angles larger than 90°. The analyzing power A_y is identically zero since the matrix elements are all real valued.

The effect of the self-energy is shown by the dotted lines. The self-energy is parametrized using the values for $\alpha(p^2)$ as given in Table I. An excellent fit to the observed cross sections is obtained. At energies exceeding 150 MeV, where the *D*-wave contribution to the cross section is dominant, this parameter efficiently enhances the cross section at θ_γ larger than 90°. At 100 MeV the effect of $\alpha(p^2)$ on the cross section is only minor, probably reflecting the dominance of electric radiation at these energies. The parameter $\alpha(p^2)$ has been chosen real for simplicity. Taking complex values for it strongly affects A_y and a good fit to both cross section and analyzing power at 200 MeV could be obtained, but since this would introduce another free parameter in the fit, we have not explored this freedom further.

Curiously enough, the values for $\alpha(p^2)$ given in Table I show a resonance like trend with the maximum near the pion production threshold. This suggests that the phenomenological parameter $\alpha(p^2)$ might be related to the virtual production of the pion in the $pd \rightarrow {}^3\mathrm{He}\gamma$ process. In a model for the

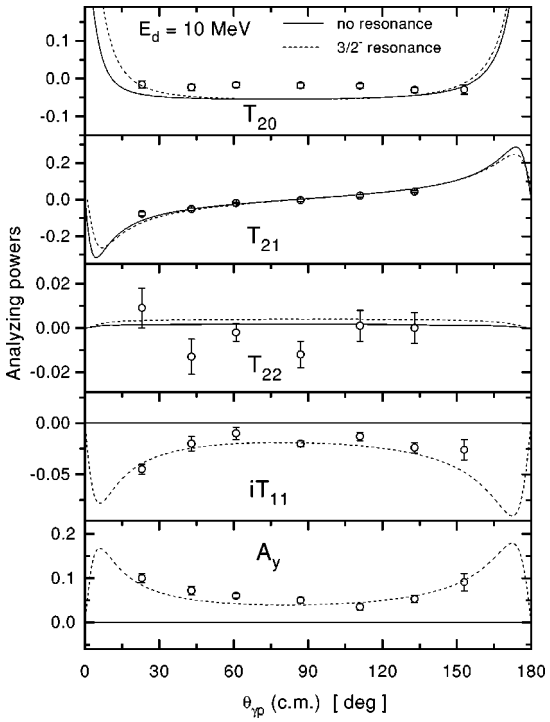

FIG. 5. Deuteron analyzing powers T_k and proton analyzing power A_y at the deuteron laboratory energy 10 MeV. Data are from [41]. Solid lines show results of the default calculation for the wave function [19]; dashed lines include the $\frac{3}{2}^-$ resonance with excitation energy 14 MeV and width 10 MeV.

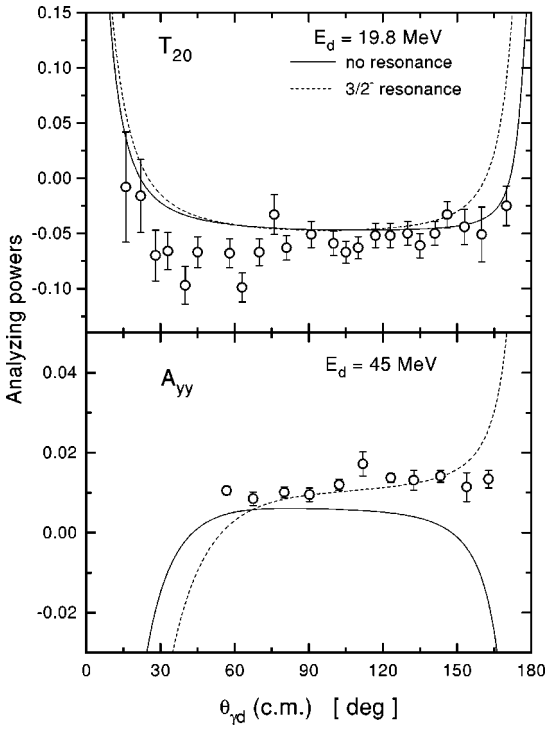

FIG. 6. Deuteron tensor analyzing powers at deuteron laboratory energies 19.8 and 45 MeV. Data are from [42] and [11], respectively. Notation for the curves is the same as in Fig. 5.

^{3}He self-energy where the ^{3}He propagator is dressed with pion loops, the imaginary part of the self-energy grows linearly with the pion momentum starting at the threshold. Application of a dispersion relation results in a cusplike structure, at the same position, for the real part of the self-energy. This could explain the peak observed in the fitted values of $\alpha(p^2)$. However, in preliminary calculations using a simple one-pion loop model, the order of magnitude of the peak was not reproduced.

The inclusion of *pd* rescattering has a relatively small effect on the calculated cross section (dashed curves). As argued above, it is of crucial importance for the vector analyzing power. As is shown in Fig. 4 a reasonable agreement is obtained for A_y at 200 MeV. The agreement for A_y at other energies is unfortunately not as good, and results are not shown. The reason is probably that at 200 MeV the *S* and the *D* components of the WF are both large and of comparable magnitude. Since for A_y relative phases between the matrix elements for different spin projections are important, the calculation is rather accurate at this energy. At lower energies the cross section is dominated by the *S* wave, and contributions, which have relatively small effects on the cross section, will strongly affect A_y.

In Fig. 5 we present the deuteron analyzing powers T_k and the proton analyzing power A_y at small deuteron energy 10 MeV (the equivalent proton energy is 5 MeV). The default calculation (without self-energy and phase shifts), shown by the solid lines, gives a reasonable description for all T_k, except iT_{11} for which the calculation predicts zero. Including the $\frac{3}{2}^-$ resonance, where we take $G_1(s)G_2(s)=-1$, gives quite a good agreement for iT_{11}, and A_y as well (see two lower panels in Fig. 5). This indicates that the *pd* interaction in the $\frac{3}{2}^-$ state may be responsible for the typical behavior of the vector analyzing powers iT_{11} and A_y at small energies.

Results for T_{20} and $A_{yy}=(-1/\sqrt{2})T_{20}-\sqrt{3}T_{22}$ at higher energies are shown in Fig. 6. The strength of the resonance has been chosen the same as in Fig. 5 (though, in general, it may depend on the energy). This contribution affects A_{yy} at backward angles and, in particular, changes the trend of A_{yy} at 45 MeV.

In the experiments disscused above neither the proton, deuteron, or ^{3}He contribution was close to the corresponding pole; i.e., the intermediate states in the diagrams on Fig. 1 are always far off shell. The cross section is therefore a result of an interference between different terms in the total amplitude.

It is also of interest to test the model in conditions where either the proton or the deuteron contribution dominates. These conditions are realized in experiments on the electrodisintegration of ^{3}He, where either the proton or the deuteron is detected in coincidence with the electron. Figure 7 presents the exclusive cross sections for the $^3\mathrm{He}(e,e'p)d$ and the $^3\mathrm{He}(e,e'd)p$ reactions.

The $^3\mathrm{He}(e,e'p)d$ experiments with detection of the proton have been performed at Saclay [44] and NIKHEF [43]. The experimental arrangement is such that the energy-momentum transfer is kept constant while the angle between knocked-out proton and $\vec{q}$ varies. The WF of ^{3}He is probed at high missing momentum (the deuteron recoil momentum) $p_{\mathrm{mis}}=|\vec{p}_1-\vec{q}|>230$ MeV (NIKHEF) and 300 MeV (Saclay). Our calculation (two top panels in Fig. 7) overpredicts the experiment at 250 MeV$<p_{\mathrm{mis}}<$450 MeV and gives

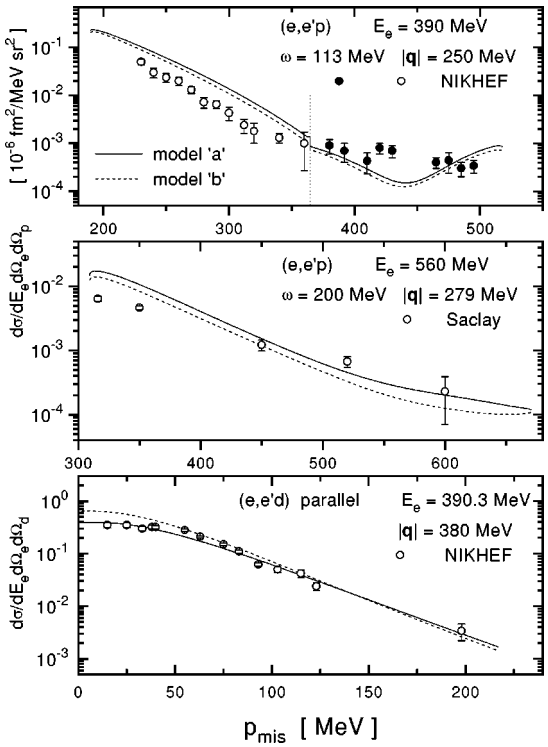

FIG. 7. Cross sections for the ^{3}He electrodisintegration: two upper panels show the $(e,e'p)$ reaction in (q,ω) kinematics; lower panel, $(e,e'd)$ reaction in parallel kinematics. Discontinuity in the upper panel shows the change in the calculation from ''left'' to ''right'' kinematics which corresponds to the conditions of the NIKHEF experiment [43]. Data in the middle and the bottom are from [44] and [45], respectively. Solid (dashed) lines are the default calculations with the wave function from [19] ([16]).

a reasonable description at higher $p_{\rm mis}$. Inclusion of the self-energy in the ^{3}He propagator and the *pd* phase shifts has a minor effect and does not improve the agreement.

Calculations of this reaction have also been performed in Refs. [6,46,47] in a nonrelativistic framework. In [6] the *pd* interaction has been included; however, no better agreement with the data was obtained (Fig. 13 in [6]). A good description of the NIKHEF data has been achieved in [47], where the inital and final $3N$ states are calculated exactly in the Faddeev approach. Based on these calculations, we can conclude that the above discrepancy in Fig. 7 may be due to neglect of *off-shell pd* rescattering in our model.

At the NIKHEF kinematics [45] for the ^{3}He$(e,e'd)p$ reaction (lower panel in Fig. 7) the deuteron is detected in the direction of $\vec{q}$, and as the energy transfer approximately corresponds to quasifree knock-out of the deuteron (i.e., $q_0 \approx \vec{q}^2/2m_2$), the deuteron contribution is enhanced. In this kinematics one probes only two response functions (RFs), $W_T(s,q^2,\theta_\gamma=0)$ and $W_L(s,q^2,\theta_\gamma=0)$, where s and q^2 vary. The missing momentum $p_{\rm mis}=|\vec{p}_2-\vec{q}|$ (the momentum of the recoil proton) varies from $\approx$ 10 to 200 MeV. As is seen from Fig. 7 (lower panel) the two models for the ^{3}He WF give different results, in particular, the WF of ''b'' yields larger cross section at small $p_{\rm mis}$. In these conditions the $^1S_0$ diagram also becomes important. On the whole, the description of these data with the Argonne v18 WF (model ''a'') is good.

From the two models of the ^{3}He WFs which have been used, the one calculated with the Argonne v18 NN interaction [19] gives better overall agreement with the ^{3}He$(e,e'd)p$ and *pd* capture data.

Finally we note that in [20] the capture reaction for the timelike virtual photons (e^+e^- production) has been studied in the same approach. We checked that the inclusion of the ^{3}He self-energy or *pd* phase shifts has a small effect on the response functions the dilepton production. Only the transverse response function is influenced to the same extent as the cross section for real photons.

V. CONCLUSIONS

A covariant and gauge-invariant model for the reactions $p+d\leftrightarrow{}^3$He$+\gamma^*$ has been developed. The model is a generalization of the approach [16] to higher energies, and is based on the assumption of the dominance of the radiation from the external particle lines. An important element of the model is an additional internal amplitude needed to ensure gauge invariance. The contribution of this amplitude is sizable, especially for real photons.

Results of calculations have been compared with experiments for the radiative *pd* capture and the electrodisintegration of ^{3}He. Some of the results for the $\gamma+{}^3$He$\rightarrow p+d$ have been presented in a previous publication [20].

In general, the model seems to account for the basic mechanism of these reactions over a wide range of energies. In order to improve the description of the capture cross section at high energies 100–500 MeV, additional mechanisms have been included. In particular the introduction of a self-energy correction in the ^{3}He propagator leads to a redistribution of the strength in the angular dependence of the cross sections and brings the calculation very close to the data. This effect has been included via a phenomenological parameter $\alpha(p^2)$, which appears to have a resonancelike dependence as a function of the proton energy, peaking at the pion-production threshold. Eventhough this is suggestive, we were unable to reproduce this feature in a simple one-pion loop calculation for the ^{3}He self-energy.

The imaginary part of the amplitude has been generated through the *pd* scattering phase shifts as required by unitarity arguments. Only rescattering in the $\frac{1}{2}^+$ channel has been included. This allows us to reproduce the proton analyzing power A_y at $T_p=200$ MeV; however, we failed at energies 100 and 150 MeV. At small energies, $T_d=10$ MeV, 19.8 MeV, and 45 MeV, the approach describes tensor analyzing powers T_{20}, T_{21}, and T_{22} resonably well. The vector analyzing powers iT_{11} and A_y are reproduced by including the $\frac{3}{2}^-$ resonance with the excitation energy 14 MeV and width 10 MeV. With only a single strength parameter an excellent description of both iT_{11} and A_y at 10 MeV is obtained.

Comparison with the ^{3}He$(e,e'd)p$ reaction shows an almost perfect agreement between the calculation and the NIKHEF data in parallel kinematics. For the ^{3}He$(e,e'p)d$ reaction in the (q,ω) kinematics description of the experiment is worse, especially at missing momenta less than 400 MeV. This shortcoming, which is probably related to the ''off-shell'' rescattering effects which have been neglected in our model, remains to be investigated in detail.

ACKNOWLEDGMENTS

We thank R.B. Wiringa for providing us with wave function of ^{3}He. We would also like to thank A.E.L. Dieperink and R.G.E. Timmermans for useful discussions, and E. J. Beise for sending the deuteron form factors. Numerous discussions with J. Ryckebusch and his comments are gratefully acknowledged. This work was supported by the Fund for Scientific Research-Flanders (FWO-Vlaanderen) and the Foundation for Fundamental Research on Matter (FOM) of the Netherlands.

APPENDIX A: γdd HALF-OFF-SHELL VERTEX

The fully-off-shell e.m. vertex function for the spin-1 particle was considered in Ref. [14]; it contains 14 independent functions $g_i(p'^2,p^2,q^2)$. We are interested in the half-off-shell vertex corresponding to the initial particle on shell and final particle off shell. In this case the vertex becomes

$$\begin{aligned}\Gamma^{\rho\alpha\mu}(p',p)\xi_\alpha=&\{g^{\rho\alpha}[(p+p')^\mu g_1-q^\mu g_2]+[q^\rho g^{\mu\alpha}-q^\alpha g^{\mu\rho}]g_3-[q^\rho g^{\mu\alpha}+q^\alpha g^{\mu\rho}]g_4\\&-[q^\alpha g^{\mu\rho}+(p+p')^\rho g^{\mu\alpha}]g_5-[q^\alpha g^{\mu\rho}-(p+p')^\rho g^{\mu\alpha}]g_6-p'^\rho q^\alpha[(p+p')^\mu(g_7-g_8)\\&+q^\mu(g_{10}-g_9)]+p^\rho q^\alpha[-(p+p')^\mu(g_{11}+g_{12})+q^\mu(g_{13}+g_{14})]\}\xi_\alpha,\end{aligned}\tag{A1}$$

where $q=p-p'$ and the conditions $p^2=m^2$ and $p\cdot\xi=0$ have been used. There are ten independent combinations of functions $g_i(p'^2,m^2,q^2)$ in this equation, we denote them $f_i(p'^2,m^2,q^2)$, where $f_i=g_i$ for $i=1,\ldots,6$, $f_7=g_7-g_8$, $f_{10}=g_{10}-g_9$, $f_{11}=g_{11}+g_{12}$, and $f_{14}=g_{13}+g_{14}$.

Charge conjugation imposes the relations[1] $g_i(p'^2,p^2,q^2)=g_i(p^2,p'^2,q^2)$ for $i=1,3,6,7,10,11,12$ and $g_i(p'^2,p^2,q^2)=-g_i(p^2,p'^2,q^2)$ for $i=2,4,5,8,9,13,14$. These relations are of particular importance for the on-mass-shell case ($p^2=p'^2=m^2$), as they result in the constraints

$$g_2=g_4=g_5=g_8=g_9=g_{13}=g_{14}=0.\tag{A2}$$

Correspondingly one has

$$\begin{aligned}f_2(m^2,m^2,q^2)&=f_4(m^2,m^2,q^2)\\&=f_5(m^2,m^2,q^2)\\&=f_{14}(m^2,m^2,q^2)=0,\end{aligned}\tag{A3}$$

and using the condition $\xi'^*\cdot p'=0$ one recovers the on-shell vertex

$$\begin{aligned}\xi'^*_\rho\Gamma^{\rho\alpha\mu}(p',p)\xi_\alpha=\xi'^*_\rho[&g^{\rho\alpha}(p+p')^\mu f_1\\&+(q^\rho g^{\mu\alpha}-q^\alpha g^{\mu\rho})(f_3+f_6)\\&-q^\rho q^\alpha(p+p')^\mu f_{11}]\xi_\alpha.\end{aligned}\tag{A4}$$

The functions $f_{1,3,6,11}(m^2,m^2,q^2)$ can further be identified with the deuteron e.m. form factors in Eq. (7):

$$f_1(m^2,m^2,q^2)=-F_1(q^2),\tag{A5}$$

$$f_3(m^2,m^2,q^2)+f_6(m^2,m^2,q^2)=F_2(q^2),$$

$$f_{11}(m^2,m^2,q^2)=-\frac{F_3(q^2)}{2m^2}.$$

[1] In [14] f_{14} is erroneously indicated as an even function and f_{12} as an odd one.

For the half-off-shell vertex in Eq. (A1) one has to impose the WT identity Eq. (6). The latter takes the form

$$\begin{aligned}&g^{\rho\alpha}[q\cdot(p+p')f_1-q^2f_2]\\&\quad+p'^\rho q^\alpha[2f_4+2f_6-q\cdot(p+p')f_7-q^2f_{10}]\\&\quad+p^\rho q^\alpha[-2f_4-2f_5-q\cdot(p+p')f_{11}+q^2f_{14}]\\&\quad=-g^{\rho\alpha}q\cdot(p+p')+p'^\rho q^\alpha.\end{aligned}\tag{A6}$$

As a consequence the following relations for $f_i(p'^2,m^2,q^2)$ hold:

$$q\cdot(p+p')(1+f_1)-q^2f_2=0,$$

$$2f_4+2f_5+q\cdot(p+p')f_{11}-q^2f_{14}=0,\tag{A7}$$

$$2f_4+2f_6-q\cdot(p+p')f_7-q^2f_{10}=1.\tag{A8}$$

Note that $q\cdot(p+p')=m^2-p'^2$, and this product vanishes on shell. As a result of Eq. (A3), Eqs. (A7) are trivially satisfied when $p'^2=m^2$. From Eq. (A8) we get the additional constraint (when putting $p'^2=m^2$)

$$2f_6(m^2,m^2,q^2)-q^2f_{10}(m^2,m^2,q^2)=1\tag{A9}$$

and, from the second equation in Eqs. (A5),

$$f_3(m^2,m^2,q^2)=F_2(q^2)-\frac{1}{2}-\frac{q^2}{2}f_{10}(m^2,m^2,q^2).\tag{A10}$$

Now we neglect the dependence of f_1, f_3, f_6, f_7, f_{10}, f_{11}, and f_{14} on the off-shell variable p'^2. Using Eqs. (A7), (A8), and (A5) we find the remaining functions

$$f_2(p'^2,m^2,q^2)=q\cdot(p+p')\frac{1-F_1(q^2)}{q^2},$$

$$f_4(p'^2,m^2,q^2)=\frac{1}{2}q\cdot(p+p')f_7(p'^2,m^2,q^2),$$

$$f_4(p'^2,m^2,q^2)+f_5(p'^2,m^2,q^2)=\frac{1}{2}q\cdot(p+p')\frac{F_3(q^2)}{2m^2}. \tag{A11}$$

In this way all functions are expressed in terms of the on-shell form factors and the functions f_7 and f_{10} which remain unconstrained.

The off-shell vertex takes the form

$$\begin{aligned}\Gamma^{\rho\alpha\mu}(p',p)\xi_\alpha=\Bigg\{&-g^{\rho\alpha}(p+p')^\mu+p'^\rho g^{\mu\alpha}+g^{\rho\alpha}[(p+p')^\mu q^2-q\cdot(p+p')q^\mu]\frac{1-F_1(q^2)}{q^2}+(q^\rho g^{\mu\alpha}-q^\alpha g^{\mu\rho})F_2(q^2)\\&+\left[p^\rho q^\alpha(p+p')^\mu-\frac{1}{2}[q^\alpha g^{\mu\rho}+(p^\rho+p'^\rho)g^{\mu\alpha}]q\cdot(p+p')\right]\frac{F_3(q^2)}{2m^2}+p'^\rho[-q^\alpha(p+p')^\mu\\&+g^{\mu\alpha}q\cdot(p+p')]f_7(m^2,m^2,q^2)+p'^\rho(q^2g^{\mu\alpha}-q^\mu q^\alpha)f_{10}(m^2,m^2,q^2)\Bigg\}\xi_\alpha.\end{aligned} \tag{A12}$$

Contributions from f_7 and f_{10} are gauge invariant themselves and it is not possible to fix them without microscopic calculations. It is seen that the f_{10} term gives no contribution for real photons and we put it equal to zero. We will also make the assumption $f_7=F_3(q^2)/2m_2^2$, which allows one to obtain the quadrupole part in the simpler form

$$\left[q^\rho q^\alpha(p+p')^\mu-\frac{1}{2}(q^\alpha g^{\mu\rho}+q^\rho g^{\mu\alpha})q\cdot(p+p')\right]\frac{F_3(q^2)}{2m^2}. \tag{A13}$$

Finally, we arrive at the vertex in Eq. (5) of Sec. II A. This vertex reduces to the on-mass-shell form when $p'^2=m^2$ and satisfies the half-off-shell WT identity.

APPENDIX B: GAUGE-INVARIANT AMPLITUDE

In this appendix we present the expression for the total amplitude.

It is convenient first to separate the convection current and the normal magnetic moment current of the proton. One can use the identity

$$\begin{aligned}&(\not p_1-\not q-m_1)\gamma^\mu u(\vec p_1,\lambda_p)\\&\quad=[(2p_1-q)^\mu+(q^\mu-\not q\gamma^\mu)]u(\vec p_1,\lambda_p).\end{aligned} \tag{B1}$$

A similar identity can be applied to the ^{3}He term.

For further convenience we introduce the notation ($i=1,2,3$)

$$\phi_\pm^\alpha(i)=[\gamma^\alpha G_\pm(Q_i^2)-Q_i^\alpha H_\pm(Q_i^2)]\gamma_5 \tag{B2}$$

and ($i=1,2$)

$$\hat\phi_+^\alpha(i)=[\gamma^\alpha G_+(Q_i^2)-Q_3^\alpha H_+(Q_i^2)]\gamma_5, \tag{B3}$$

where the difference between ϕ_+ and $\hat\phi_+$ is only in the term proportional to H_+.

After adding the internal amplitude $M_{\rm int}(1)+M_{\rm int}(2)$ to $M_{\rm ext}$ we obtain the total amplitude in the form $M=A_1+A_2+A_3$.

The effective proton contribution A_1 takes the form

$$\begin{aligned}A_1^{\mu\alpha}=&\phi_+^\alpha(1)\frac{(2p_1-q)^\mu}{D_1}\\&-\hat\phi_+^\alpha(1)\frac{M_r}{m_1}\frac{[2Q_3-(M_r/m_1)q]^\mu}{(Q_1^2-Q_3^2)}\\&+g^{\mu\alpha}\frac{M_r}{m_1}H_+(Q_1^2)\gamma_5+\phi_+(1)\\&\times\left[\frac{q^\mu-\not q\gamma^\mu}{D_1}+S(p_1-q,m_1)\right.\\&\left.\times\left(-i\frac{\sigma^{\mu\nu}q_\nu}{2m_1}F_2(q^2)+\tilde\Gamma^\mu\right)\right]\\&+\phi_-^\alpha(1)\frac{1}{2m_1}\left[-i\frac{\sigma^{\mu\nu}q_\nu}{2m_1}F_2(q^2)+\tilde\Gamma^\mu\right],\end{aligned} \tag{B4}$$

where $D_1=(p_1-q)^2-m_1^2$ and $\tilde\Gamma^\mu\equiv\tilde F_1(q^2)(q^\mu\not q-q^2\gamma^\mu)$.

The effective ^{3}He contribution reads

$$A_3^{\mu\alpha}=\left[2\frac{(2p_3+q)^\mu}{D_3}+\frac{M_r}{m_1}\frac{[2Q_3-(M_r/m_1)q]^\mu}{(Q_1^2-Q_3^2)}-\frac{M_r}{m_2}\frac{[2Q_3+(M_r/m_2)q]^\mu}{(Q_2^2-Q_3^2)}\right]\phi_+^\alpha(3)+\left[2\frac{-q^\mu+\gamma^\mu\not{q}}{D_3}+\left(-i\frac{\sigma^{\mu\nu}q_\nu}{2m_3}F_2(q^2)+2\tilde{\Gamma}^\mu\right)\times S(p_3+q,m_3)\right]\phi_+^\alpha(3)+\left[-i\frac{\sigma^{\mu\nu}q_\nu}{2m_3}F_2(q^2)+2\tilde{\Gamma}^\mu\right]\frac{1}{2m_3}\phi_-^\alpha(3), \quad \text{(B5)}$$

with $D_3=(p_3+q)^2-m_3^2$ and the same notation for $\tilde{\Gamma}^\mu$ as in Eq. (B4).

Finally, the effective deuteron contribution can be written in the form

$$A_2=A_2(\mathrm{ch})+A_2(\mathrm{mag})+A_2(\mathrm{quad}), \quad \text{(B6)}$$

with charge, magnetic, and quadrupole terms given, respectively, by

$$A_2^{\mu\alpha}(\mathrm{ch})=\left[\frac{(2p_2-q)^\mu}{D_2}-\tilde{F}_1(q^2)\left(\frac{(2p_2-q)^\mu}{D_2}q^2+q^\mu\right)\right]\times\left[\frac{q^\alpha}{m_2^2}\phi_+(2)\cdot(p_2-q)+\phi_+^\alpha(2)\right]+g^{\mu\alpha}\left[\frac{\phi_+(2)\cdot(p_2-q)}{m_2^2}-\frac{M_r}{m_2}H_+(Q_2^2)\gamma_5\right]+\frac{M_r}{m_2}\frac{[2Q_3+(M/m_2)q]^\mu}{Q_2^2-Q_3^2}\hat{\phi}_+^\alpha(2), \quad \text{(B7)}$$

$$A_2^{\mu\alpha}(\mathrm{mag})=\frac{F_2(q^2)}{D_2}(q^\rho g^{\mu\alpha}-q^\alpha g^{\mu\rho})\times\left[\frac{(p_2-q)_\rho}{m_2^2}\phi_+(2)\cdot(p_2-q)-\phi_+(2)_\rho\right], \quad \text{(B8)}$$

and

$$A_2^{\mu\alpha}(\mathrm{quad})=\frac{F_3(q^2)}{2m_2^2}\left[\frac{(2p_2-q)^\mu}{D_2}q^\rho q^\alpha+\frac{1}{2}(q^\alpha g^{\mu\rho}+q^\rho g^{\mu\alpha})\right]\times\left[\frac{(p_2-q)_\rho}{m_2^2}\phi_+(2)\cdot(p_2-q)-\phi_+(2)_\rho\right]. \quad \text{(B9)}$$

In the above formulas $D_2=(p_2-q)^2-m_2^2$ and

$$\phi_+(2)\cdot(p_2-q)=[(m_1+m_3)G_+(Q_2^2)-(p_2-q)\cdot Q_2 H_+(Q_2^2)]\gamma_5. \quad \text{(B10)}$$

It is now straightforward to verify that all terms are separately gauge invariant, i.e., satisfy the requirements $q_\mu A_i^{\mu\alpha}=0$ for $i=1,2,3$.

APPENDIX C: CROSS SECTIONS AND ANALYZING POWERS

We use standard kinematics for the reaction $p+d\to{}^3\mathrm{He}+\gamma^*$. In particular, for virtual photons the orientation of the lepton plane is determined by the out-of-plane angle ϕ with respect to the reaction plane. Calculations for the *pd* capture are performed in the center-of-mass frame and those for electron scattering in the laboratory frame of the ^{3}He.

First we define the RFs, which contain all hadronic information, as follows:

$$W_T=\frac{1}{6}\sum_{\mathrm{polar}}(|J_x|^2+|J_y|^2), \quad W_L=\frac{1}{6}\frac{|q^2|}{q_0^2}\sum_{\mathrm{polar}}|J_z|^2,$$

$$W_{TT}=\frac{1}{6}\sum_{\mathrm{polar}}(|J_y|^2-|J_x|^2),$$

$$W_{LT}=-\frac{1}{6}\frac{\sqrt{|q^2|}}{q_0}\sum_{\mathrm{polar}}2\sqrt{2}\,\mathrm{Re}(J_zJ_x^*), \quad \text{(C1)}$$

where q_0 is the (virtual) photon energy, and the components of the e.m. current $J^\mu\equiv\bar{u}(\vec{p}_3,\lambda_h)M^{\mu\alpha}u(\vec{p}_1,\lambda_p)\xi_\alpha(\lambda_d)$ are evaluated in the system with the *OZ* axis along $\vec{q}$. In these expressions gauge invariance has been used to eliminate the charge component of the current. Note that RFs depend on three variables, $W_i=W_i(s,q^2,\theta_\gamma)$, where θ_γ is the photon angle with respect to the proton direction and $s=(m_1+m_2)^2+2m_2T_p$ is the invariant energy. These definitions are chosen to be consistent with definitions used previously in [23,26,20] for the production of e^+e^- pairs. In the latter case q^2 in Eq. (C1) is positive.

The $p+d\to{}^3\mathrm{He}+\gamma$ cross section then reads

$$\frac{d\sigma}{d\Omega_\gamma}=\frac{\alpha m_1m_3q_c'}{4\pi p_cs}W_T(s,0,\theta_\gamma), \quad \text{(C2)}$$

where $q_c'=(s-m_3^2)/2\sqrt{s}$ stands for the real photon momentum, p_c is the proton c.m. momentum, and α is the fine-structure constant.

In terms of RFs one can also express the cross section for the reaction $e+{}^3\mathrm{He}\to e'+p+d$. The cross section for $^3\mathrm{He}(e,e'd)p$ in the laboratory frame is (see, e.g., [36])

$$\frac{d\sigma}{dE_{e'}d\Omega_{e'}d\Omega_{d'}}=\frac{\sigma_M m_1|\vec{p}_2|}{16\pi^3m_3f_{\mathrm{rec},d}}(S_Tv_T+S_Lv_L+S_{TT}v_{TT}\cos2\phi+S_{LT}v_{LT}\cos\phi). \quad \text{(C3)}$$

Here σ_M is the Mott cross section, $f_{\mathrm{rec},d}=|1+(|\vec{p}_2|q_0-E_2|\vec{q}|\cos\theta_d)/|\vec{p}_2|m_3|$ is the recoil factor, θ_d is the angle between the photon and deuteron momenta, and the electron kinematical factors are [36]

$$v_T=\frac{1}{2}\lambda+\tan^2\frac{\theta_e}{2},\quad v_L=\lambda^2,\quad v_{TT}=-\frac{1}{2}\lambda,$$

$$v_{LT}=-\frac{\lambda}{\sqrt{2}}\left(\lambda+\tan^2\frac{\theta_e}{2}\right)^{1/2},\quad \lambda\equiv\frac{|q^2|}{\vec{q}^2}. \tag{C4}$$

The $^3\mathrm{He}(e,e'p)d$ cross section is calculated from Eq. (C3) using the relation

$$\frac{d\sigma}{dE_{e'}d\,\Omega_{e'}d\,\Omega_{p'}}=\frac{d\,\sigma}{d\,E_{e'}d\,\Omega_{e'}d\,\Omega_{d'}}\frac{|\vec{p}_1|f_{\mathrm{rec},d}}{|\vec{p}_2|f_{\mathrm{rec},p}}, \tag{C5}$$

with the corresponding recoil factor $f_{\mathrm{rec},p}=|1+(|\vec{p}_1|q_0-E_1|\vec{q}|\cos\theta_p)/|\vec{p}_1|m_3|$.

RFs in electron scattering S_i are traditionally defined [36] somewhat differently from Eq. (C1). Using time reversal one can obtain the relations

$$S_T=3W_T,\quad S_L=3\frac{\vec{q}^2}{|q^2|}W_L,$$

$$S_{TT}=3W_{TT},\quad S_{LT}=-3\frac{|\vec{q}|}{\sqrt{|q^2|}}W_{LT}, \tag{C6}$$

between the two sets of RFs, where factor of 3 accounts for the deuteron spin degeneracy.

It is convenient to introduce the following set of polarization vectors for the timelike or spacelike photon (where the OZ axis is along $\vec{q}$):

$$\epsilon^*(\pm1)=\frac{1}{\sqrt{2}}(0,\mp1,i,0),\quad \epsilon^*(0)=\frac{1}{\sqrt{|q^2|}}(|\vec{q}|,0,0,q_0), \tag{C7}$$

and for the deuteron (moving in the direction specified by the unit vector $\vec{n}_2$)

$$\vec{\xi}(\lambda)=\left[\frac{|\vec{p}_2|}{m_2}[\vec{n}_2\cdot\vec{\xi}(\lambda)],\vec{\xi}(\lambda)+\vec{n}_2\left(\frac{E_2(\vec{p}_2)}{m_2}-1\right)[\vec{\xi}(\lambda)\cdot\vec{n}_2]\right],$$

$$\vec{\xi}(\pm1)=\frac{1}{\sqrt{2}}(\mp1,-i,0),\quad \vec{\xi}(0)=(0,0,1). \tag{C8}$$

Here the helicity states are specified by $\lambda=\pm1,0$. These vectors satisfy the Lorentz condition, Eq. (2), are mutually orthogonal, and are normalized as follows: $\xi^*(\lambda_d)\cdot\xi(\lambda_d)=-1$ (for all λ_d), $\epsilon^*(\lambda_\gamma)\cdot\epsilon(\lambda_\gamma)=-1$ (for $\lambda_\gamma=\pm1$), and $\epsilon^*(0)\cdot\epsilon(0)=-q^2/|q^2|$.

Using Eq. (C7) we can rewrite RFs in Eq. (C1) through the products of the current J with $\epsilon^*(\lambda)$:

$$|J_x|^2+|J_y|^2=|J\cdot\epsilon^*(+1)|^2+|J\cdot\epsilon^*(-1)|^2,$$

$$|J_y|^2-|J_x|^2=2\,\mathrm{Re}\{J\cdot\epsilon^*(+1)[J\cdot\epsilon^*(-1)]^*\},$$

$$\frac{|q^2|}{q_0^2}|J_z|^2=|J\cdot\epsilon^*(0)|^2,$$

$$\frac{\sqrt{|q^2|}}{q_0}\sqrt{2}\,\mathrm{Re}(J_zJ_x^*)=\frac{q^2}{|q^2|}\mathrm{Re}\{J\cdot\epsilon^*(0)[J\cdot\epsilon^*(-1)-J\cdot\epsilon^*(+1)]^*\}, \tag{C9}$$

where use has been made of current conservation. These relations in particular show that the RFs defined in Eq. (C1) are Lorentz invariant.

To calculate the RFs S_i for electron scattering in the laboratory frame one can first calculate W_i in the c.m. frame and then use Eq. (C6).

Finally, we will need the following analyzing powers for vector polarized proton beam:

$$A_y=i\sum_{\lambda_d,\lambda_h,\lambda_\gamma}(M_{\lambda_p=-1}M^*_{\lambda_p=+1}-M_{\lambda_p=+1}M^*_{\lambda_p=-1})S^{-1}, \tag{C10}$$

and tensor- and vector-polarized deuteron beams

$$T_{20}=\frac{1}{\sqrt{2}}\sum_{\lambda_p,\lambda_h,\lambda_\gamma}\{|M_{\lambda_d=+1}|^2+|M_{\lambda_d=-1}|^2-2|M_{\lambda_d=0}|^2\}S^{-1}, \tag{C11}$$

$$T_{22}=\sqrt{3}\sum_{\lambda_p,\lambda_h,\lambda_\gamma}(M_{\lambda_d=-1}M^*_{\lambda_d=+1})S^{-1}, \tag{C12}$$

$$T_{21}=\sqrt{\frac{3}{2}}\sum_{\lambda_p,\lambda_h,\lambda_\gamma}(M_{\lambda_d=0}M^*_{\lambda_d=-1}-M_{\lambda_d=+1}M^*_{\lambda_d=0})S^{-1}, \tag{C13}$$

$$iT_{11}=i\sqrt{\frac{3}{2}}\sum_{\lambda_p,\lambda_h,\lambda_\gamma}(M_{\lambda_d=0}M^*_{\lambda_d=+1}+M_{\lambda_d=-1}M^*_{\lambda_d=0})S^{-1}, \tag{C14}$$

where

$$S=\sum_{\lambda_p,\lambda_h,\lambda_\gamma,\lambda_d}|M_{\lambda\gamma\lambda_h,\lambda_p\lambda_d}|^2. \tag{C15}$$

These expressions are consistent with definitions of Ref. [37] (Chap. 4).

[1] J.P. Didelez, H. Langevin-Joliot, Z. Maric, and V. Radojevic, Nucl. Phys. **A143**, 602 (1970).
[2] B.A. Craver, Y.E. Kim, and A. Tubis, Nucl. Phys. **A276**, 237 (1977).
[3] B.F. Gibson and D.R. Lehman, Phys. Rev. C **11**, 29 (1975).
[4] S. Aufleger and D. Drechsel, Nucl. Phys. **A364**, 81 (1981).
[5] V.V. Kotlyar and A.V. Shebeko, Yad. Fiz. **54**, 698 (1991) [Sov. J. Nucl. Phys. **54**, 423 (1991)].
[6] E. van Meijgaard and J.A. Tjon, Phys. Rev. C **42**, 96 (1990).
[7] W. Schadow and W. Sandhas, Phys. Rev. C **55**, 1074 (1997).
[8] W. Schadow and W. Sandhas, Nucl. Phys. **A631**, 588c (1998); Phys. Rev. C **59**, 607 (1999).
[9] W. Sandhas, W. Schadow, G. Ellerkmann, L.L. Howell, and S.A. Sofianos, Nucl. Phys. **A631**, 210c (1998).
[10] J.M. Laget, in *New Vistas in Electro-Nuclear Physics*, edited by E. L. Tomusiak, H. S. Caplan, and E. T. Dressler (Plenum Press, New York, 1986), p. 361.
[11] H. Anklin *et al.*, Nucl. Phys. **A636**, 189 (1998).
[12] W. Glöckle, H. Kamada, J. Golak, and H. Witala, nucl-th/9807017.
[13] F.E. Low, Phys. Rev. **110**, 974 (1958).
[14] B. Sakita, Phys. Rev. **127**, 1800 (1962).
[15] J. Govaerts, J.L. Lucio, A. Martinez, and J. Pestieau, Nucl. Phys. **A368**, 409 (1981).
[16] G. Fäldt, and L.-G. Larsson, J. Phys. G **19**, 171 (1993).
[17] R. Schiavilla, V.R. Pandharipande, and R. Wiringa, Nucl. Phys. **A449**, 219 (1986).
[18] R.B. Wiringa, V.G.J. Stoks, and R. Schiavilla, Phys. Rev. C **51**, 38 (1995).
[19] J.L. Forest, V.R. Pandharipande, S.C. Pieper, R.B. Wiringa, R. Schiavilla, and A. Arriaga, Phys. Rev. C **54**, 646 (1996); http:www.phy.anl.gov/theory/research/overlap.
[20] A. Yu. Korchin, D. Van Neck, M. Waroquier, O. Scholten, and A. E. L. Dieperink, Phys. Lett. B **441**, 17 (1998).
[21] S.I. Nagorny, Yu.A. Kasatkin, E.V. Inopin, and I.K. Kirichenko, Sov. J. Nucl. Phys. **49**, 465 (1989).
[22] S.I. Nagorny, Yu.A. Kasatkin, V.A. Zolenko, and I.K. Kirichenko, Sov. J. Nucl. Phys. **55**, 1325 (1992).
[23] D. Van Neck, A.E.L. Dieperink, and O. Scholten, Nucl. Phys. **A574**, 643 (1994).
[24] F. Gross and D.O. Riska, Phys. Rev. C **36**, 1928 (1987).
[25] R. Arnold, C.E. Carlson, and F. Gross, Phys. Rev. C **21**, 1426 (1980).
[26] A.Yu. Korchin and O. Scholten, Nucl. Phys. **A581**, 493 (1995).
[27] M. Gourden *et al.*, Nuovo Cimento **37**, 524 (1965).
[28] W.W. Buck and F. Gross, Phys. Rev. D **20**, 2361 (1979).
[29] G.E. Brown, Mannque Rho, and W. Weise, Nucl. Phys. **A454**, 669 (1986); M. Gari and W. Krumpelmann, Z. Phys. A **322**, 689 (1985); R. Williams, S. Krewald, and K. Linen, Phys. Rev. C **51**, 566 (1995).
[30] J.S. McCarthy, I. Sick, and R.R. Whitney, Phys. Rev. C **15**, 1396 (1977).
[31] R. Machleidt, Adv. Nucl. Phys. **19**, 189 (1989).
[32] J. Hockert, D.O. Riska, M. Gari, and A. Huffman, Nucl. Phys. **A217**, 14 (1973).
[33] K. Nakayama, in *Perspectives in the Structure of Hadronic Systems*, edited by M. N. Harakeh, J. H. Koch, and O. Scholten, Vol. 333 of NATO Advanced Studies Institute, Series B: Physics (Plenum, New York, 1994).
[34] J. Arvieux, Nucl. Phys. **A221**, 253 (1974).
[35] A. Niiler *et al.*, Phys. Rev. C **1**, 1342 (1970).
[36] T. W. Donnelly, in *New Vistas in Electro-Nuclear Physics* [10], p. 151.
[37] B. A. Robson, *The Theory of Polarization Phenomena* (Clarendon Press, Oxford, 1974), p. 119.
[38] M.J. Pickar *et al.*, Phys. Rev. C **35**, 37 (1987).
[39] J.M. Cameron *et al.*, Nucl. Phys. **A424**, 549 (1984).
[40] S.I. Nagorny, Yu. A. Kasatkin, and V.A. Zolenko, Phys. Lett. B **316**, 231 (1993).
[41] F. Goeckner, W.K. Pitts, and L.D. Knutson, Phys. Rev. C **45**, 2536 (1992).
[42] G.J. Schmid *et al.*, Phys. Rev. C **53**, 35 (1996).
[43] P.H.M. Keizer *et al.*, Phys. Lett. B **197**, 29 (1987).
[44] C. Marchand *et al.*, Phys. Rev. Lett. **60**, 1703 (1988).
[45] P.H.M. Keizer *et al.*, Phys. Lett. B **157**, 255 (1985).
[46] J.M. Laget, Phys. Lett. B **199**, 493 (1987).
[47] J. Golak, H. Kamada, H. Witala, W. Glöckle, and S. Ishikawa, Phys. Rev. C **51**, 1638 (1995).